EXPERIMENTAL CARDIOLOGY: ORIGINAL ARTICLE

Remodelling of cardiac gap junction connexin 43 and arrhythmogenesis

Takashi Mayama MD[1], Ken Matsumura MD[1], Hai Lin PhD[2], Koichi Ogawa PhD[3], Issei Imanaga MD PhD FIACS[4]

T Mayama, K Matsumura, H Lin, K Ogawa, I Imanaga. Remodelling of cardiac gap junction connexin 43 and arrhythmogenesis. Exp Clin Cardiol 2007;12(2):67-76.

BACKGROUND: In cardiac muscle, the gap junction plays a pivotal role in electrical cell-to-cell coupling and impulse propagation between cells. The function of the gap junction depends on the regulation of connexin in the gap junction channel. A dysfunction of the gap junction is possibly caused by the downregulation of connexin or one of arrhythmogenic factors. The mechanisms of ventricular fibrillation, a lethal tachyarrhythmia, have been studied in relation to the remodelling of connexin.

OBJECTIVES: To determine what type of connexin 43 (Cx43) remodelling contributes to the generation of ventricular fibrillation and what factors induce the modelling of Cx43.

METHODS: Aconitine-induced ventricular fibrillation was induced in hearts isolated from adult rats. Alterations in the electrical activity, the phosphorylation of Cx43 and the expression of Cx43 were evaluated by both intracellular and extracellular recording of the action potentials, Western blotting and immunohistochemistry, respectively. Flutter activity after the application of aconitine shifted spontaneously to fibrillation, showing an electrical interaction between neighbouring cells in close proximity to one another. The facility of the shift from flutter to fibrillation was evaluated as a susceptibility of the heart to fibrillation in relation to gap junction function. The effects of phorbol 12-myristate 13-acetate, angiotensin II (AII) analogues, AII antagonists, the diabetic state, protein kinase A (PKA) activator, cyclic AMP analogues, d-sotalol (class III antiarrhythmic drug) and PKA inhibitors

on the susceptibility of the heart to fibrillation were examined.

RESULTS: Pathological hearts with heterogeneous expression of Cx43 at the gap junction, such as phorbol 12-myristate 13-acetate- and AII analogue-treated hearts, as well as diabetic hearts, showed a significantly higher susceptibility to fibrillation. On the other hand, hearts with augmentative expression of Cx43 at the gap junction, such as hearts pretreated with a PKA activator, a cyclic AMP analogue (8-bromo-cyclic AMP) or d-sotalol, showed a significantly lower susceptibility to fibrillation. At the beginning of fibrillation, an increase in the cardiac tissue AII level, an augmentation of the protein kinase C (PKC)-epsilon activity, the presence of PKC-mediated hyperphosphorylation, a suppression of the PKA-mediated phosphorylation of Cx43 and a reduction in the expression of Cx43 at the gap junction were observed. These alterations in Cx43 expression were also observed to increase as the fibrillation advanced.

CONCLUSIONS: Augmentation of PKC-mediated phosphorylation and suppression of PKA-mediated phosphorylation induces the downward remodelling of Cx43. Such remodelling of Cx43 induces asynchronous electrical activities and makes the ventricular tissue susceptible to fibrillation. PKC is activated by AII. The fibrillation itself remodels Cx43, thereby causing a vicious cycle. As a result, PKC inhibitors, AII antagonists and PKA activators are considered to possibly have a protective effect against the initiation or advancement of ventricular fibrillation.

Key Words: *Cardiac gap junction; PKA-mediated phosphorylation; PKC-mediated phosphorylation; Remodelling of connexin 43; Ventricular fibrillation*

In cardiac muscle, it is generally accepted that the gap junction greatly contributes to electrical cell-to-cell coupling and impulse propagation between cells, because the electrical resistance of the gap junction is much lower than that of the surface membrane (1) and the gap junction channel is permeable to large molecules (2,3). The function of the gap junction fundamentally depends on the characteristics of connexin that form the gap junction channel, including such factors as the number of functional channels, the opening and closing of the channel, the phosphorylation of connexin, the expression of connexin and the distribution of connexin. It has been reported that the remodelling of connexin essentially contributes to an arrhythmogenic substrate (4-6).

Ventricular fibrillation is the most lethal type of all known tachyarrhythmias. Several factors, such as abnormalities of the ionic channels of the active membrane and the re-entry of excitation, which is caused by a slow conduction or acceleration of

anisotropic conduction, are involved in the mechanisms that cause the generation of fibrillation. These two factors are possibly induced by the downward remodelling of connexin. A direct relationship between susceptibility of the heart to arrhythmogenesis and remodelling of connexin should thus be elucidated to clarify the contribution of the gap junction to the generation of fibrillation.

Aconitine, a type of alkaloid, is known to be seriously toxic to cardiac muscle cells and also induces cardiac fibrillation. In this regard, characteristics of aconitine-induced cardiac fibrillation have been previously reported (7-9); it has also been used as a model of cardiac fibrillation in in vitro experiments. The regular and rapid electrical activity of the heart, namely, the flutter induced after the application of aconitine, is then spontaneously followed by irregular and rapid electrical activity, ie, fibrillation, while also demonstrating the appearance of intercellular electrical interaction. The interaction of electrical activity between

neighboring cells, which is induced by the micro-re-entry of excitation, is possibly caused by a dysfunction of the gap junction. It is therefore conceivable that the generation of fibrillation is triggered by a dysfunction of the gap junction.

The present study focused on how alterations in the expression and phosphorylation of connexin 43 (Cx43), which is predominantly expressed in ventricular cells, affect the susceptibility of the heart to aconitine-induced fibrillation, and also attempted to clarify how fibrillation itself remodels Cx43. Part of this study was previously reported in a preliminary form (10).

METHODS

Animals and extraction of the heart

Adult, male Wistar rats with a mean (± SEM) weight of 235.5±15.2 g were used. For the type 1 (insulin-dependent diabetes mellitus [IDDM]) diabetic model, streptozotocin (STZ)-induced diabetic rats were used. These rats were in a diabetic state with a blood glucose level higher than 400 mg/dL by four to five weeks after the injection of STZ 50 mg/kg in a single intravenous dose (11). For the type 2 (noninsulin-dependent diabetes mellitus [NIDDM]) diabetic model, genetically diabetic Otsuka Long-Evans Tokushima Fatty (OLETF) rats (Otsuka Pharmaceuticals Co Ltd, Japan) were used (Long-Evans Tokushima Otsuka [LETO] rats were used as controls). These rats were in a diabetic state with a blood glucose level higher than 300 mg/dL, four months after birth. Age-matched animals were used as a normal control group. They were sacrificed by a blow to the head, and the experimental protocol was carried out according to the method approved by the Institutional Animal Care and Use Committee of Fukuoka University (Fukuoka, Japan). The animals were given intraperitoneal injections of heparin (Heparin Novo, Novo Nordik A/S, Denmark) at a dose of 1000 U/kg, 30 min before they were sacrificed.

Recording of the transmembrane action potentials

Thin endocardial muscle strips (less than 1 mm in thickness, 10 mm to 15 mm in length and 2 mm to 3 mm in width) were isolated from the right ventricular wall after removal of the heart from the animal. These were fixed in a perfusion chamber (0.4 mL in volume) and irrigated with well-oxygenated standard Krebs solution (NaCl, 130 mmol/L; KCl, 5.4 mmol/L; NaHCO$_3$, 11.9 mmol/L; NaH$_2$PO$_4$, 1.2 mmol/L; MgCl$_2$, 1.2 mmol/L; CaCl$_2$, 2.5 mmol/L; glucose, 5.5 mmol/L; saturated with a gas mixture of 97% O$_2$ and 3% CO$_2$, and adjusted to a pH of 7.4) at a constant flow (5 mL/min) and at a constant temperature (37°C). The preparation was thereafter electrically stimulated with a threshold strength at 4 Hz using a suction electrode. The transmembrane action potentials were then recorded by two or three conventional glass microelectrodes placed at a distance of 200 μm from each other.

Recording of the monophasic action potentials

The hearts, excised quickly from the animal, were mounted on a Langendorff apparatus and were then perfused with well-oxygenated standard Krebs solution at a constant pressure (60 mmHg). After 10 to 15 min of stabilization, the monophasic action potentials were recorded with suction electrodes placed on the surface of either the right or left ventricle, which showed spontaneous beating at 200 beats/min to 300 beats/min.

Immunoblotting and immunohistochemistry

After 10 to 15 min of stabilization, the isolated hearts mounted on the Langendorff apparatus were perfused with Krebs solution, including reagents. At the beginning of fibrillation, at an advanced stage of fibrillation (after 20 min of fibrillation) and after treatment with reagents, the ventricular tissue specimens were removed from the Langendorff apparatus and subjected to Western blotting and immunohistochemistry. The tissue samples were frozen in liquid nitrogen for Western blotting or were immersed in fixing solutions (3% buffered paraformaldehyde) for immunohistochemistry.

The phosphorylation of Cx43 was evaluated by Western blotting using mouse monoclonal anti-Cx43 antibody as a primary antibody (lot number 19100924, Chemicon International Inc, USA) and anti-mouse immunoglobulin G (IgG) as a secondary antibody (lot number 145660, Amersham Pharmacia Biotech, United Kingdom), or the rabbit polyclonal anti-Cx43 antibody as a primary antibody (lot number 41191365, Zymed Laboratories Inc, USA) and anti-rabbit IgG as a secondary antibody (lot number 21020094, Chemicon International Inc). The total amount of Cx43 was evaluated by the mean density of the total band detected using the mouse monoclonal anti-Cx43 antibody as a primary antibody (lot number 40387290, Zymed Laboratories Inc) and anti-mouse IgG as a secondary antibody (lot number NA 931, Amersham Pharmacia Biotech). The procedures for Western blotting and the evaluation of the phosphorylation of Cx43 have been previously described (11,12).

For the immunohistochemistry of Cx43, the rabbit polyclonal anti-Cx43 antibody was used as a primary antibody (lot number 30476831, Zymed Laboratories Inc), and goat anti-rabbit IgG was used as a secondary antibody (Alexa Fluor 488, Lot number 35068A, Molecular Probes, USA). The expression of immunoreactive spots of Cx43 at the intercalated disk and localization of Cx43 were evaluated by immunohistochemistry. Immunofluorescence was detected by confocal laser scan microscopy (LSM-410, Carl Zeiss, Germany) on the preparations sliced to 10 μm in thickness. The procedures for immunohistochemistry and analysis of immunofluorescence have been previously described (11,12).

Measurement of tissue angiotensin II

The expression of angiotensin II (AII) in cardiac tissue was evaluated by Western blotting using rabbit anti-AII and IgG (lot number 419835, Phoenix Pharmaceuticals Inc, USA).

Identification of isoforms of protein kinase C

The identification of protein kinase C (PKC) isoforms was performed by Western blotting using a polyclonal antibody for PKC-α (C-20, sc-208, lot number G032), PKC-β$_1$ (C-16, sc-209, lot number E222), PKC-β$_2$ (C-18, sc-210, lot number I1602), PKC-δ (C-17, sc-213, lot number G012), PKC-ε (C-15, sc-214, lot number J1503) and PKC-θ (C-18, sc-212, lot number I2502) (Santa Cruz Biotechnology Inc, USA).

Chemicals and reagents

The following agents were used: aconitine (lot number 045K1002, Sigma-Aldrich, USA), cyclic AMP analogue (8-bromo-adenosine 3′,5′-cyclic monophosphate sodium salt, lot number 85H7808, Sigma-Aldrich), protein kinase A (PKA) activator (Sp-adenosine 3′,5′-cyclic monophosphothioate triethylamine salt, a potent membrane-permeable activator of cyclic AMP-dependent protein kinase I and II, lot number 97H4681, Sigma-Aldrich), PKA inhibitor (Rp-adenosine 3′,5′-cyclic monophosphothioate triethylamine salt, a specific membrane-permeable inhibitor of cyclic AMP-dependent protein kinase I
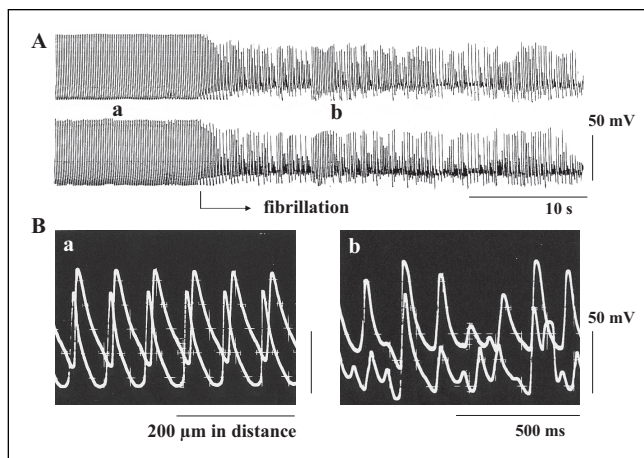
Figure 1) *The transmembrane action potentials recorded from an endocardial muscle strip isolated from the right ventricle of the rat heart. Two glass microelectrodes were placed 200 μm apart from each other. **A** Slow record; **B** Fast record. **a** and **b** indicate the action potentials at the flutter stage and the fibrillation stage, respectively. Both flutter and fibrillation were induced by the application of aconitine at a concentration of 0.1 μmol/L*

Figure 2) *The monophasic action potentials recorded from the surface of the right ventricle of the isolated rat heart with a suction electrode. The heart was perfused on a Langendorff apparatus. The upper and the lower traces represent the output and the action potentials, respectively. Both flutter and fibrillation were induced by the application of aconitine at a concentration of 0.1 μmol/L*

and II (lot number 087H4643, Research Biochemicals International, USA), phorbol 12-myristate 13-acetate (PMA) (lot number 38F0185, Sigma-Aldrich), calphostin C (lot number 087H4652, Research Biochemicals International) as a PKC inhibitor, leupeptin (acetyl-leu-leu-arg-al) (lot number 080K8613, Sigma-Aldrich) as a lysosomal inhibitor, N-acetyl-leu-leu-norleucinal (lot number 91K1603, Sigma-Aldrich) as a proteasomal inhibitor, d-sotalol (class III antiarrhythmic drug, donated by Dr Mordechai Manoach, Tel Aviv Med, Israel), [Asn[1],Val[5]]-AII acetate salt (lot number 053K51282, Sigma-Aldrich) as an AII agonist, [Sar[1],Ile[8]]-AII (lot number 410314, Peptide Institute Inc, Japan) as an AII receptor antagonist and [Sar[1],Val[5],Ala[8]]-AII (saralasin) (lot number 1/11725, Tocris, USA) as an AII antagonist. These reagents were dissolved in either distilled water or DMSO as the stock solution, were frozen and were dissolved in Krebs solution at the final concentrations described above just before use.

Densitometry
The mean density of the Cx43 complex isoforms in the immunoblots, and the mean fluorescent intensity and area of immunoreactive spots for Cx43 on the confocal laser scan micrographs were analyzed by the National Institutes of Health (USA) Image software program.

Statistical analysis
The data are presented as the mean ± SEM. Unpaired Student's *t* tests were used to analyze the statistical significance (P<0.001) between the means.

RESULTS
Aconitine-induced flutter and fibrillation
Aconitine was applied to the isolated muscle strip driven electrically at 4 Hz at a final concentration of 0.1 μmol/L, while electrical activity was monitored by recording the transmembrane action potentials. Approximately 5 min after the application of aconitine, automatic activity appeared, and at this stage, the electrical stimulation was discontinued and aconitine was
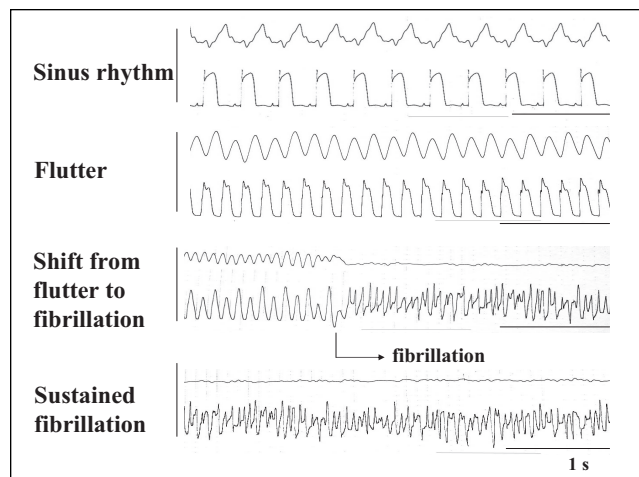
washed out. Thereafter, the automatic activity gradually became more rapid, and flutter, which showed action potentials with a regular amplitude in the range of 100 mV to 110 mV and a regular firing frequency in the range of 7 Hz to 8 Hz, was induced; it was followed by fibrillation even in the absence of aconitine (Figure 1). In the preparation from the normal heart, a mean of 8.0±0.8 min later, the membrane was slightly depolarized, and the flutter shifted spontaneously to fibrillation, with an irregular amplitude and an irregular frequency (Figure 1). At the beginning of and during such fibrillation, the various kinds of action potentials, with a range of 20 mV to 60 mV in amplitude and a range of 20 V/s to 30 V/s in the maximum rate of rise, were included in the electrical activity of a myocyte, and these irregular electrical activities were simultaneously recorded from the neighboring cells 200 μm apart (Figure 1B). These findings suggest that fibrillation is generated by an electrical interaction between adjacent cells through dysfunctional gap junctions that are incompletely inhibited.

Despite the absence of aconitine, the fibrillation became advanced and continued for approximately 30 min. When a very low concentration (0.1 mmol/L) of heptanol was administrated during the flutter, the flutter shifted promptly to fibrillation within several seconds. Such a low concentration of heptanol did not essentially affect the rate of rise in the action potential but induced an incomplete activation of the gap junction communication, namely, dysfunction of the gap junction (13). This is further described in the Discussion section.

In experiments using the Langendorff method, aconitine, at a final concentration of 0.1 μmol/L, was applied to the heart showing spontaneous sinus rhythm at 200 beats/min to 300 beats/min, while the electrical activity was monitored by recording the monophasic action potentials. Approximately 5 min later, the sinus rhythm gradually accelerated, and at this stage, the aconitine was washed out. Thereafter, tachycardia, at a regular rhythm of 400 beats/min to 500 beats/min, which is called flutter, was generated, and it was followed by fibrillation (Figure 2). The flutter shifted spontaneously to fibrillation,
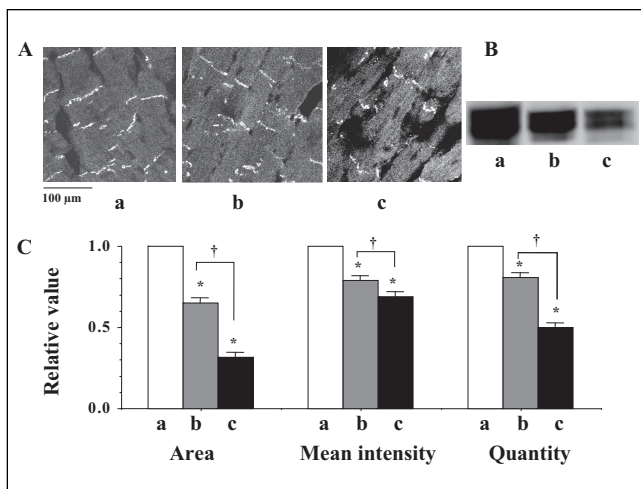
Figure 3) A *Confocal laser scan micrographs of the immunofluorescence of connexin 43 (Cx43).* **a**, **b** *and* **c** *indicate the micrographs before fibrillation (control), at the beginning of fibrillation and during advanced fibrillation (after 20 min), respectively.* **B** *Western blots of Cx43 using a monoclonal antibody for Cx43 (Zymed Laboratories Inc, USA) in the ventricle of the rat heart.* **C** *A statistical analysis of the immunofluorescence and Western blots of Cx43 – a comparison of the area, the mean intensity of the immunoreactive signals at the gap junction and the quantity of Cx43; the columns represent the relative value (1.0 is the value of the control [a]), and the vertical bars represent the mean ± SEM. *P<0.001 versus the control (a); †P<0.001*

Figure 4) A *Western blots of connexin 43 (Cx43) using a polyclonl antibody for Cx43 (Zymed Laboratories Inc, USA) in the ventricle of the rat heart.* **a**, **b** *and* **c** *indicate the signal before fibrillation (control), at the beginning of fibrillation and during advanced fibrillation (after 20 min), respectively.* **B** *A statistical analysis of the Western blots – a comparison of the P1 to P0 ratio among the control (**a**) and the two fibrillation (**b** and **c**) stages; the columns represent the relative value (1.0 is the value of the control [**a**]), and the vertical bars represent the mean ± SEM. *P<0.001 versus the control (a); †P<0.001*

showing action potentials with an irregular amplitude and rhythm, within a mean of 8.5±1.5 min in the normal hearts. A low concentration of heptanol (0.1 mmol/L) rapidly and remarkably shifted the flutter to fibrillation within several seconds, in the same manner as observed in in vitro experiments. The fibrillation was thereafter sustained for approximately 30 min, despite the absence of aconitine (Figure 2).

Alterations in the expression of Cx43 at the gap junction during fibrillation
At the beginning of fibrillation, just after the shift from flutter to fibrillation, a confocal image (by immunohistochemistry) revealed a heterogeneous expression of Cx43 at the gap junction (Figure 3Ab). Western blots showed a decrease in the quantity of Cx43 (Figure 3Bb). Both the immunoreactive area and the mean intensity of immunoreactive signals for Cx43 were observed to decrease (Figure 3Ac), in addition to the quantity of Cx43, as the fibrillation advanced (Figure 3Ac and 3Bc). A statistical analysis of time-dependent alterations in the expression of Cx43 is shown in Figure 3C.

Alterations in the phosphorylation of Cx43 during fibrillation
Two distinct isoforms were detected in the Western blots of Cx43 (using rabbit polyclonal anti-Cx43 antibody). It was previously confirmed that the lower molecular isoform (P0) was an unphosphorylated molecule, while the higher molecular isoform (P1) was a PKA-mediated phosphorylated molecule (12). The P1 to P0 ratio was thus evaluated to determine the status of the PKA-mediated phosphorylation of Cx43. Alterations in the P1 to P0 ratio in terms of the progression of fibrillation are shown in Figure 4B. The PKA-mediated phosphorylation of Cx43 was suppressed at the beginning of
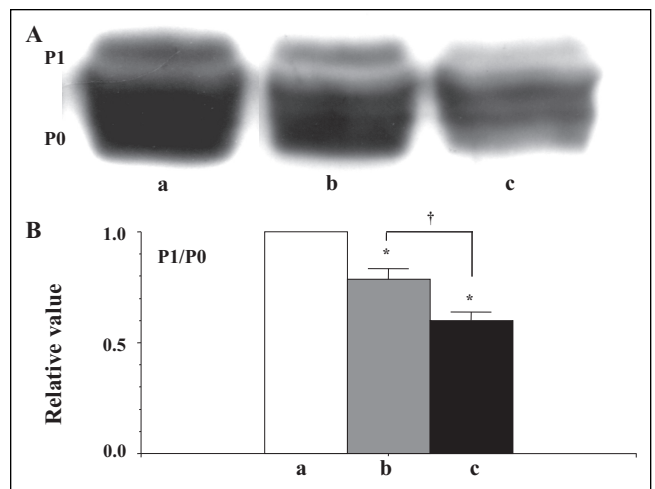
fibrillation, and the dephosphorylation of Cx43 thereafter became enhanced as the fibrillation advanced (Figure 4).

Three distinct isoforms were detected by the Western blots of Cx43 (using a mouse monoclonal anti-Cx43 antibody from Chemicon International Inc). It was also confirmed that the lower molecular isoform (P0) was an unphosphorylated molecule and that the higher molecular isoform (P2) was the PKC-mediated phosphorylated molecule (11). The P2 to P0 ratio was evaluated as the status of the PKC-mediated phosphorylation of Cx43. Alterations in the P2 to P0 ratio in terms of the progression of the fibrillation are shown in Figure 5B. At the beginning of fibrillation, the PKC-mediated phosphorylation of Cx43 was augmented, and as fibrillation continued, hyperphosphorylation was enhanced (Figure 5).

Isoform of PKC activated during fibrillation
PKC-ε was activated at the beginning of fibrillation, and the activation was enhanced as fibrillation continued (Figure 6). No other isoforms of PKC-α, -β₁, -β₂, -δ and -θ significantly changed compared with the control heart (not shown here).

Cardiac tissue level of AII
An increase in the cardiac tissue level of AII was observed at the beginning of fibrillation, and it was enhanced as the fibrillation continued (Figure 6).

Factors influencing the time of the shift from flutter to fibrillation
Absolute times are summarized in Table 1.
Effects of PMA: Sixty minutes after the perfusion of PMA at a concentration of 0.1 µmol/L, immunoreactive signals of
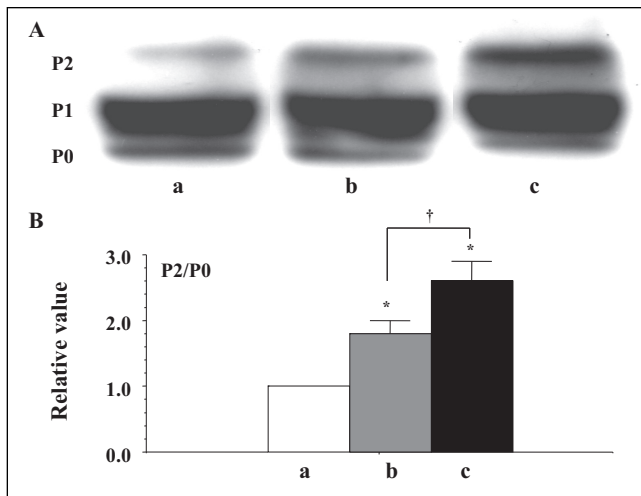
Figure 5) A *Western blots of connexin 43 (Cx43) using a monoclonal antibody for Cx43 (Chemicon International Inc, USA) in the ventricle of the rat heart.* **a**, **b** *and* **c** *indicate the signal before fibrillation (control), at the beginning of fibrillation and during advanced fibrillation (after 20 min), respectively.* **B** *A statistical analysis of the Western blots – a comparison of the P2 to P0 ratio among the control (**a**) and the two fibrillation (**b** and **c**) stages; the columns represent the relative value (1.0 is the value of the control [**a**]), and the vertical bars represent the mean ± SEM.* *P<0.001 versus the control (a); †P<0.001

Figure 6) A *Western blots of protein kinase C (PKC)-ε and cardiac tissue angiotensin II (AII).* **a**, **b** *and* **c** *indicate the signal before fibrillation (control), at the beginning of fibrillation and during advanced fibrillation (after 20 min), respectively.* **B** *A statistical analysis of the Western blots – a comparison of PKC-ε and AII among the control (**a**) and the two fibrillation (**b** and **c**) stages; the columns represent the relative value (1.0 is the value of the control [**a**]), and the vertical bars represent the mean ± SEM.* *P<0.001 versus the control (a); †P<0.001

Cx43 at the gap junction were heterogeneous (namely, there was a decrease in the area and the mean intensity) (Figure 7), and the quantity of Cx43 decreased in association with PKC-mediated hyperphosphorylation (increase in the P2 to P0 ratio) (Figures 8 and 9). In PMA-treated hearts, the mean time of the shift from flutter to fibrillation was significantly shortened to 1.5±0.3 min.

These effects of PMA were abolished by the PKC inhibitor calphostin C (1.0 µmol/L) and the lysosomal inhibitor leupeptin (25 µmol/L) (Table 1).

Type 1 (STZ-induced) and type 2 (OLETF) models of diabetic hearts: In the STZ-induced diabetic hearts, the heterogeneous expression of Cx43 was observed at the gap junction (namely, a decrease in the area and the mean intensity of immunoreactive signals of Cx43) (Figures 7B, 10Ab and 10C). A reduction in the quantity of Cx43 was also observed in association with PKC-mediated hyperphosphorylation (increase in the P1 to P0 ratio) (Figures 8, 9 and 10Bb). In these diabetic hearts, the decrease in Cx43 expression was remarkably enhanced as fibrillation advanced (Figures 10Ac, 10Ad, 10Bc and 10Bd). In the STZ-induced diabetic rat heart, the time of the shift significantly decreased to a mean of 2.1±0.4 min, and this effect was thereafter abolished by calphostin C (1.0 µmol/L), AII antagonists (1.0 µmol/L), leupeptin (25 µmol/L) and the proteasomal inhibitor N-acetyl-leu-leu-norleucinal (25 µmol/L) (Table 1).

In the OLETF rats, the heterogeneous expression of Cx43 was observed at the gap junction (namely, a decrease in the area and the mean intensity of the immunoreactive signals of Cx43) (Figure 7). A reduction in the amount of Cx43 was also observed (Figures 8, 9 and 10) together with an increase in PKC-mediated hyperphosphorylation (augmentation of the
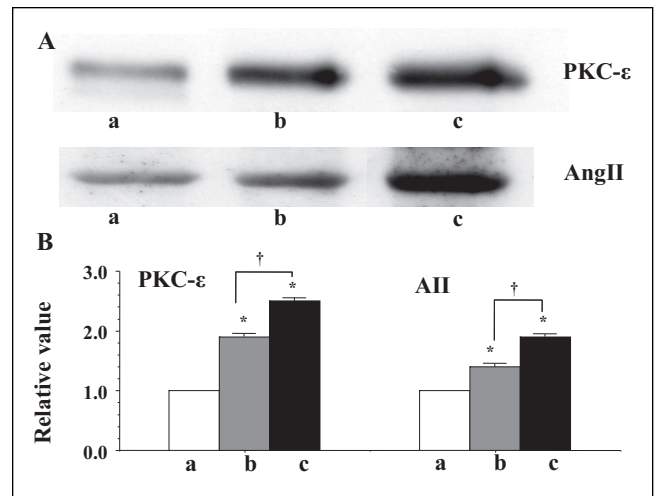
TABLE 1
Factors influencing the time of the shift from flutter to fibrillation

Factor	Time from beginning of flutter to beginning of fibrillation, min (mean ± SEM)
Control	8.5±1.5
Phorbol 12-myristate 13-acetate	1.5±0.3*
Phorbol 12-myristate 13-acetate plus calphostin C	6.7±1.5
Phorbol 12-myristate 13-acetate plus leupeptin	7.5±1.2
Type 1 diabetic model – streptozotocin	2.1±0.4*
Type 1 diabetic model – streptozotocin plus calphostin C	6.5±1.3
Type 1 diabetic model – streptozotocin plus leupeptin	6.8±1.8
Type 1 diabetic model – streptozotocin plus AII antagonist	7.1±1.5
Type 1 diabetic model – streptozotocin plus N-acetyl-leu-leu-norleucinal	6.5±2.3
Type II diabetic model – OLETF	2.3±0.9*
Control of OLETF – LETO	8.2±1.2
AII analogue	1.5±0.6*
AII analogue plus AII antagonist	6.5±1.3
Hypoxia	2.2±1.2*
Protein kinase A activator	18.1±2.1*
Cyclic AMP analogue	17.2±3.1*
Cyclic AMP analogue plus protein kinase A inhibitor	9.2±1.3
d-sotalol	15.2±3.5*
d-sotalol plus protein kinase A inhibitor	9.0±2.5
Heptanol	0.05±0.001*

Aconitine (0.1 µmol/L) was administrated to the hearts, which were being irrigated on a Langendorff apparatus. The concentrations of the reagents are described in the text. *Significant difference, P<0.001 versus the control. *AII Angiotensin II; LETO Long-Evans Tokushima Otsuka; OLETF Otsuka Long-Evans Tokushima Fatty*
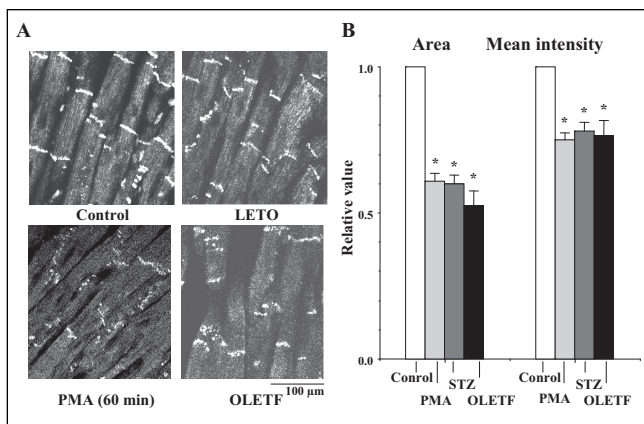
Figure 7) **A** *Confocal laser scan micrographs of the immunofluorescence of connexin 43 (Cx43) in the phorbol 12-myristate 13-acetate (PMA)-treated (0.1 µmol/L, 60 min) heart and the Otsuka Long-Evans Tokushima Fatty (OLETF) rat heart. The control had a normal condition without PMA, and the Long-Evans Tokushima Otsuka (LETO) rat heart was a control for the OLETF rat heart. Confocal micrographs of the streptozotocin (STZ)-induced diabetic rat heart are shown in Figure 10. **B** A statistical analysis of the immunofluorescence of Cx43 – a comparison of the area and the mean intensity of the immunoreactive signals at the gap junction among the control, the PMA-treated, the STZ-induced diabetic and the OLETF rat hearts; the columns represent the relative value (1.0 is the value of the control, normal and LETO hearts), and the vertical bars represent the mean ± SEM. *P<0.001 versus the control*
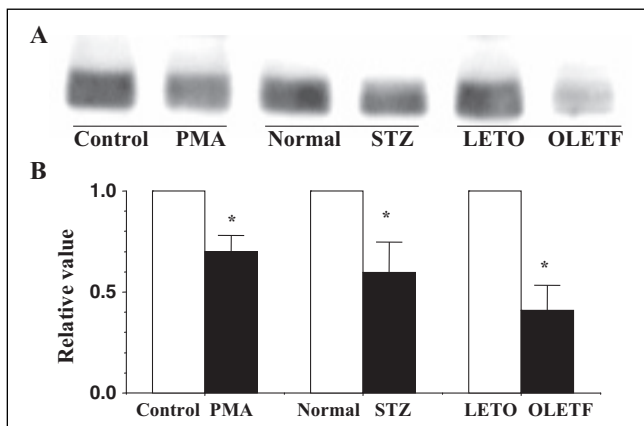

Figure 9) **A** *Western blots of connexin 43 (Cx43) using monoclonal antibody for Cx43 (Chemicon International Inc, USA) in the ventricles of the phorbol 12-myristate 13-acetate (PMA)-treated, the streptozotocin (STZ)-induced diabetic and the Otsuka Long-Evans Tokushima Fatty (OLETF) rat hearts. Control, normal and Long-Evans Tokushima Otsuka (LETO) hearts were the control hearts for the PMA-treated, the STZ-induced diabetic and the OLETF hearts, respectively. **B** A statistical analysis of the Western blots – a comparison of the P2 to P0 ratio among the PMA-treated, the STZ-induced diabetic and the OLETF rat hearts; the columns represent the relative value (1.0 is the value of the control, normal and LETO hearts), and the vertical bars represent the mean ± SEM, *P<0.001 versus the control, normal and LETO hearts*

Figure 8) **A** *Western blots of connexin 43 (Cx43) using monoclonal antibody for Cx43 (Zymed Laboratories Inc, USA) in the ventricles of the phorbol 12-myristate 13-acetate (PMA)-treated (0.1 µmol/L, 60 min), the streptozotocin (STZ)-induced diabetic and the Otsuka Long-Evans Tokushima Fatty (OLETF) rat hearts. Control, normal and Long-Evans Tokushima Otsuka (LETO) hearts were the control hearts for the PMA-treated, the STZ-induced diabetic and the OLETF hearts, respectively. **B** A statistical analysis of the Western blots – a comparison of the quantity of Cx43 among the PMA-treated, the STZ-induced diabetic and the OLETF rat hearts; the columns represent the relative value (1.0 is the value of the control, normal and LETO hearts), and the vertical bars represent the mean ± SEM. *P<0.001 versus the control, normal and LETO hearts*

P2 to P0 ratio) (Figures 8 and 9). The time of the shift was also decreased significantly (to a mean of 2.3±0.9 min) in comparison with control LETO rats (8.2±1.2 min) (Table 1).
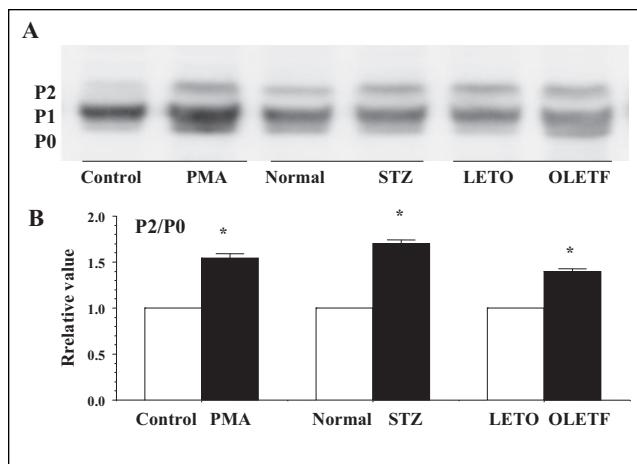**AII analogue:** Sixty minutes after perfusion of the AII analogue

(0.1 µmol/L), the time of the shift was significantly reduced to a mean of 1.5±0.6 min. This effect of the AII analogue was abolished by the AII antagonist (1.0 µmol/L) (Table 1). **PKA activator and cyclic AMP analogue:** PKA activator (1.0 µmol/L) enhanced the expression of Cx43 at the gap junction, thus showing a promotion of the immunoreactive area and the mean intensity of the immunoreactive signals of Cx43 (Figures 11Ab and 11C), as well as an increased quantity of Cx43 (Figures 11Bb and 11C). The PKA-mediated phosphorylation of Cx43 was also augmented (Figure 11Bb). In the PKA-activated hearts, the time of the shift from flutter to fibrillation was significantly prolonged and, thus, was observed to be 15 min or longer (mean 18.1±2.1 min).

Cyclic AMP analogue (8-bromo cyclic AMP) (0.5 µmol/L) showed an augmentative effect on the expression of Cx43, similar to the PKA activator (confocal image of immunohistochemistry not shown here). The time of the shift was significantly shortened (to a mean of 17.2±3.1 min). This effect of cyclic AMP analogue was abolished by PKA inhibitor (Table 1).

It was reported that a class III antiarrhythmic drug, d-sotalol, activated adenylate cyclase and increased cyclic AMP (14). Effects of d-sotalol (1.0 µmol/L) on the expression of Cx43 at the gap junction and the time to the shift were examined. In the absence of the drug, expression of Cx43 tended toward deterioration approximately 10 min after the beginning of the flutter, while in the presence of the drug, expression of Cx43 was kept almost intact, even approximately 20 min after the beginning of the flutter (Figure 12). The time of the shift was approximately 9 min in the absence of the drug, while it was prolonged to a mean of 15.2±3.5 min in the presence of the drug (Table 1). The effect of d-sotalol was inhibited by PKA inhibitor (Table 1).
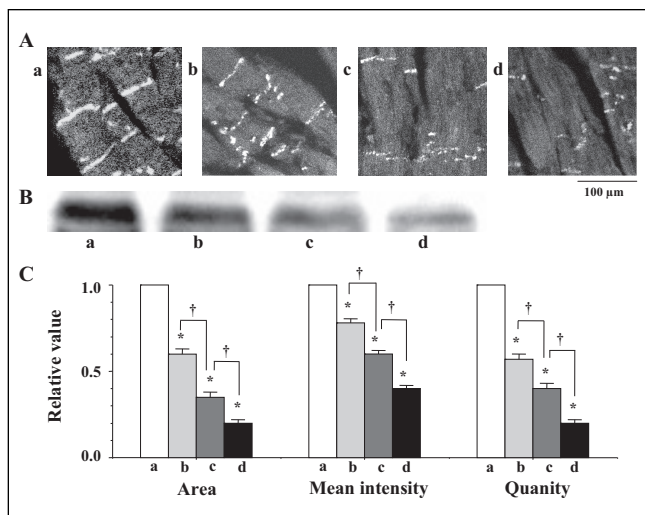
Figure 10) **A** *Confocal laser scan micrographs of the immunofluorescence of connexin 43 (Cx43) in the streptozotocin-induced diabetic rat heart.* **a**, **b**, **c** *and* **d** *indicate the micrographs of the normal (control) heart, and of the diabetic heart before fibrillation, at the beginning of fibrillation and during advanced fibrillation (after 20 min), respectively.* **B** *Western blots of Cx43 in the streptozotocin-induced diabetic rat heart.* **C** *A statistical analysis of the immunofluorescence and Western blots of Cx43 – a comparison of the area, the mean intensity of the immunoreactive signals at the gap junction and the quantity of Cx43 among* **a**, **b**, **c** *and* **d**; *the columns represent the relative value (1.0 is the value of the normal [**a**]), and the vertical bars represent the mean ± SEM. *P<0.001 versus the control; †P<0.001*
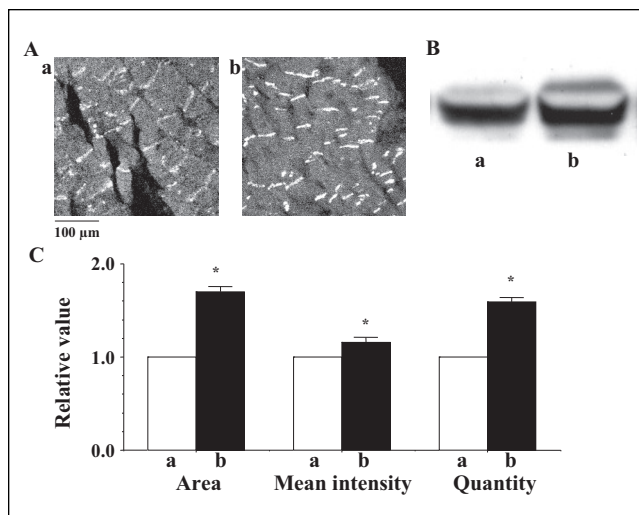

Figure 11) **A** *Confocal laser scan micrographs of the immunofluorescence of connexin 43 (Cx43) in the rat heart.* **a** *and* **b** *indicate micrographs of the control and protein kinase A activator-treated rat hearts, respectively.* **B** *Western blots using a polyclonal antibody for Cx43 (Zymed Laboratories Inc, USA) in the ventricle of the rat heart.* **C** *A statistical analysis of the immunofluorescence and Western blot findings for Cx43 – a comparison of the area, the mean intensity of the immunoreactive signals at the gap junction and the quantity of Cx43 between the control and the protein kinase A activator-treated hearts; the columns represent the relative value (1.0 is the value of the control [**a**]), and the vertical bars represent the mean ± SEM. *P<0.001 versus the control*

DISCUSSION

Aconitine is seriously toxic for cardiac cells, and it is known to induce either atrial or ventricular fibrillation. Aconitine-induced cardiac fibrillation has been well documented, and it has also been used as a model of cardiac fibrillation in in vitro experiments (7-9). The formation of ectopic pacemakers and an incomplete block of impulse conduction between cells have also been reported to be involved in the mechanism of aconitine-induced fibrillation (15). The first flutter is initiated at the stage of acceleration in ectopic pacemaker activity; the flutter then shifts spontaneously to fibrillation as time progresses. It is plausible that these processes are stimulated by the progressive intracellular Ca^{2+} overload induced by the reversed mode of Na^+-Ca^{2+} exchange activity, because aconitine increases inflow of Na^+ ions into the cell (16-18). Therefore, either an incomplete or complete block of impulse conduction associated with aconitine toxicity is caused by a dysfunction of the gap junction, because the Ca^{2+} ion is a major factor known to loosen gap junction communication due to a closure of the gap junction channel (19-22) or due to reduced expression of Cx43 at the gap junction by suppressing PKA-mediated phosphorylation (12).

At the beginning of and during fibrillation, the action potentials, with various amplitudes and differentials of rate of rise, show a mingling of electrical activity in a myocyte. This suggests that the initiation of fibrillation is triggered by the electrical interaction between neighbouring cells in close proximity to one another due to a dysfunction of the gap junction.
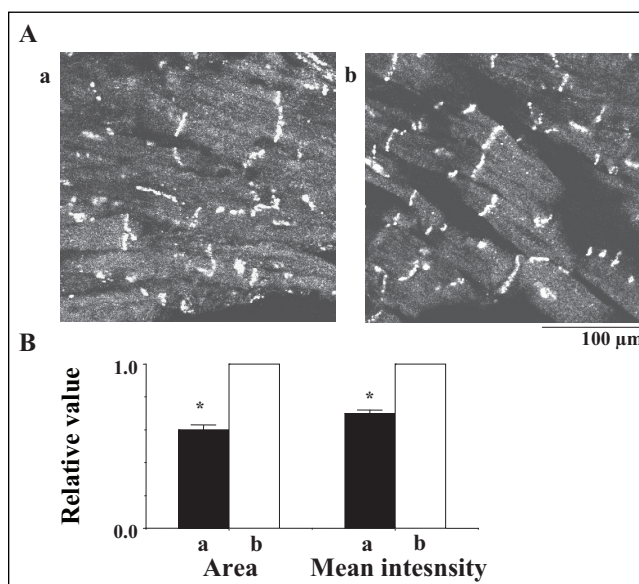

Figure 12) **A** *Confocal laser scan micrographs of the immunofluorescence of connexin 43 in the rat heart.* **a** *and* **b** *indicate micrographs 10 min after the beginning of flutter in the absence of d-sotalol and 20 min after the beginning of flutter in the presence of d-sotalol (1.0 µmol/L), respectively.* **B** *Statistical analysis of the immunofluorescence of connexin 43 – a comparison of the area and the mean intensity of the immunoreactive signals at the gap junction between* **a** *and* **b**; *the columns represent the relative value (1.0 is the value in the presence of d-sotalol [**b**]), and the vertical bars represent the mean ± SEM. P<0.001 versus* **b**

A high concentration of heptanol (higher than 1.0 mmol/L) completely closes the gap junction channels and completely inhibits electrical interaction between cells. Moreover, a high concentration of heptanol affects Na^+, K^+ and Ca^{2+} channel activities. In this condition, the critical effects of heptanol on the gap junction cannot be detected. A low concentration of heptanol (0.1 mmol/L) induces incomplete inhibition of the gap junction channels without any effects on Na^+, K^+ or Ca^{2+} channel activity (13), and accelerates electrical interaction between cells. Because a low concentration of heptanol remarkably accelerates the generation of fibrillation, unstable function of the gap junction contributes to this generation. An unstable function of the gap junction is induced by the remodelling of connexin. Moreover, in the present study, the expression of Cx43 at the gap junction was heterogeneous at the beginning of fibrillation. Such evidence suggests that the generation of the fibrillation is caused by a dysfunction of the gap junction, which thus induces a re-entrant circuit between neighbouring cells. Therefore, the facility of the shift from flutter to fibrillation is considered as an indication of the susceptibility of ventricular tissue to fibrillation in relation to the dysfunction of the gap junction.

The heart or cardiac muscle strip exposed to hypokalemia is vulnerable to ventricular fibrillation (23); diabetic or hypertrophic hearts are susceptible to hyperkalemia-induced ventricular fibrillation (24,25). This may indicate a dysfunction of the gap junction, because a K^+-deficient solution has been shown to induce intracellular Ca^{2+}-overload, while also reducing Cx43 expression at the gap junction and inducing heterogeneous morphological structure of the gap junction (23).

Therefore, according to the above considerations, the susceptibility of the heart to fibrillation is expected to be high when the expression of Cx43 at the gap junction has deteriorated. As previously reported (11) and as demonstrated in the present study, the expression of Cx43 at the gap junction region and the amount of the Cx43 protein decreased along with the PKC-mediated phosphorylation of Cx43 in the STZ-induced diabetic (type 1 diabetic model) or PMA-treated hearts. It has been proposed that the deteriorated expression of Cx43 at the gap junction in diabetic or PMA-treated hearts resulted from an acceleration of proteolytic degradation of Cx43 due to PKC-mediated hyperphosphorylation of Cx43 (11). It was demonstrated in the present study that in the type 2 diabetic model (OLETF) hearts, the expression of Cx43 at the gap junction deteriorated, while the PKC-mediated phosphorylation of Cx43 was augmented. These alterations in the expression of Cx43 are almost the same as those in the PMA-treated and the STZ-induced diabetic hearts (Figures 7, 8 and 9). The suppressed expression of Cx43 in the OLETF rats was possibly caused by an acceleration in the proteolytic degradation of Cx43 due to the PKC-mediated hyperphosphorylation of Cx43. The expression of Cx43 at the gap junction has also been previously shown to be downregulated by the suppression of the PKA-mediated phosphorylation of Cx43 (ie, dephosphorylation) in hypoxic hearts (12). In the present study, in hypoxic hearts, the time of the shift from flutter to fibrillation decreased (Table 1).

As a result, the susceptibility to develop fibrillation must be high in these pathological hearts. This hypothesis is supported by the results of the present study, in which the time of the shift from flutter to fibrillation significantly decreased in these pathological hearts compared with the normal hearts (Table 1).

Some clinical events during which irregular tachyarrhythmias show re-entry of excitation, as are often observed in diabetic, ischemic or hypoxic heart patients (26-28), may thus be explained by the results of the present study in reference to the dysfunction of the gap junction.

It was also previously demonstrated that an abnormal expression of Cx43 in the STZ-induced diabetic or the PMA-treated heart was ameliorated by treatment with a PKC inhibitor, a proteasome inhibitor or a lysosomal inhibitor (11). The higher susceptibility to fibrillation in these hearts is expected to improve by pretreatment with a PKC inhibitor, proteasome inhibitor or lysosomal inhibitor. In fact, in the present study, the short time of the shift from flutter to fibrillation in these hearts recovered to almost the same value as that of the normal hearts after the administration of these inhibitors.

At the beginning of fibrillation, the activation of PKC-ε, the PKC-mediated phosphoryaltion of Cx43 and the cardiac tissue AII level were all augmented. As a result, enhancement of the synthesis of cardiac tissue AII is suggested to contribute to the generation of fibrillation via PKC activation. This idea is supported by the fact that an AII analogue promoted the generation of fibrillation and that AII antagonists inhibited the initiation of fibrillation in the diabetic heart in which PKC was activated.

At the beginning of fibrillation, the PKC-mediated hyperphosphorylation of Cx43 and an increase in the synthesis of cardiac tissue AII were observed, along with a deterioration in the expression of Cx43 at the gap junction. The activation of PKC caused by the acceleration of AII activity was able to induce downward remodelling of Cx43. Such remodelling may therefore have produced the substrate of generation of fibrillation. These alterations were all enhanced as the fibrillation advanced. It is conceivable that the fibrillation itself remodelled Cx43.

At the beginning of fibrillation, suppression of the PKA-mediated phosphorylation of Cx43 was observed, and it was enhanced as the fibrillation advanced. This dephosphorylation of the PKA-mediated phosphorylation residue of Cx43 is possibly caused by the activation of PKC or overloaded Ca^{2+} ions, because the molecular isoform of Cx43 that is phosphorylated by PKA (P1) is inhibited by the presence of PMA (29) or Ca^{2+} ions (11).

On the other hand, when the expression of Cx43 at the gap junction is augmented, namely, the function of the gap junction is enhanced, then the susceptibility to fibrillation is expected to be low. It was previously demonstrated that a cyclic AMP analogue or PKA activator upregulated Cx43 and increased the expression of Cx43 at the gap junction (12). It was also documented in the present study that the PKA activator enhanced both the expression of Cx43 at the gap junction and the PKA-mediated phosphorylation of Cx43 (Figure 11), while also significantly prolonging the time of the shift from flutter to fibrillation in comparison with the control heart.

The dextroisomer of sotalol, d-sotalol, without beta-adrenergic receptor blocking activity, is one of the class III antiarrhythmic agents (30). There are two possibilities for

the mechanism of antiarrhythmic action of d-sotalol. One results from a prolongation of the refractory period caused by an inhibitory effect on the K^+ channel. The other is dependent on the effects of cyclic AMP or cyclic AMP-dependent activation of PKA, because d-sotalol activates adenylate cyclase and increases the intracellular cyclic AMP level (14,31). Some authors have previously reported that d-sotalol inhibited or decreased the susceptibility of the heart to develop either ventricular tachyarrhythmias or ventricular fibrillation under conditions of intracellular Ca^{2+} overload, such as during hypoxia or hypokalemia (23,32). It was proposed that intracellular Ca^{2+} overload, which suppressed gap junction communication, was either prevented or ameliorated by an acceleration of Ca^{2+} uptake into the sarcoplasmic reticulum caused by cyclic AMP (33). This idea was plausible, because cyclic AMP phosphorylates phospholamban and activates sarco/endoplasmic reticulum Ca^{2+}-ATPase (34-36). However, the promotive action of cyclic AMP or PKA by d-sotalol on the expression of Cx43 is considered to be possible. The results of the present study support d-sotalol's restorative effect on the deteriorated remodelling of Cx43, as shown in Figure 12.

CONCLUSIONS

A dysfunction of the gap junction, namely, the deteriorated expression of Cx43 at the gap junction, may contribute to the generation of fibrillation substrates. The relationship between the dysfunction of the gap junction and the generation of fibrillation is reasonably supported by the present results. The downward remodelling of Cx43 is induced by PKC-ε-mediated hyperphosphorylation of Cx43 due to activation of AII or inhibition of the PKA-mediated phosphorylation of Cx43. This remodelling of Cx43 makes the ventricular tissue susceptible to fibrillation. In addition, the fibrillation itself remodels Cx43. As a result, fibrillation may lead to a vicious cycle. It is therefore plausible that PKC inhibitors, AII antagonists or PKA activators may have protective effects against the initiation or the continuation of ventricular fibrillation.

REFERENCES

1. Weidmann S. The diffusion of radiopotassium across intercalated disks of mammalian cardiac muscle. J Physiol 1966;187:323-42.
2. Imanaga I. Cell-to-cell diffusion of procion yellow in sheep and calf Purkinje fibers. J Membr Biol 1974;16:381-8.
3. Imanaga I, Kameyama M, Irisawa H. Cell-to-cell diffusion of fluorescent dyes in paired ventricular cells. Am J Physiol 1987;252:H223-32.
4. Poelzing S, Rosenbaum DS. Altered connexin43 expression produces arrhythmia substrate in heart failure. Am J Physiol Heart Circ Physiol 2004;287:H1762-70.
5. van Rijen HV, van Veen TA, Gros D, Wilders R, de Bakker JM. Connexins and cardiac arrhythmias. Adv Cardiol 2006;42:150-60.
6. Dhein S. Role of connexins in atrial fibrillation. Adv Cardiol 2006;42:161-74.
7. Goto M, Tamai T, Yanaga T. Studies on the appearance and termination of aconitine-induced atrial fibrillation with microelectrodes. Jpn J Physiol 1963;13:196-207.
8. Imanaga I. Effects of some ions and drugs on the aconitine-induced fibrillation of the Purkinje fibers. Jpn Circ J 1967;31:1819-31.
9. Sawanobori T, Adeniya H, Hirano Y, Hiraoka M. Effects of antiarrhythmic agents and Mg^{2+} on aconitine-induced arrhythmias. Jpn Heart J 1996;37:709-18.
10. Imanaga I, Hai L, Ogawa K. Remodeling of gap junction connexin in atrial and ventricular fibrillation. In: Hiraoka M, Ogawa S, Kodama I, Inoue H, Kasanuki H, Katoh T, eds. Advances in Electrocardiology. Singapore: World Scientific, 2004:242-5.
11. Lin H, Ogawa K, Imanaga I, Tribulova N. Remodeling of connexin 43 in the diabetic rat heart. Mol Cell Biochem 2006;290:69-78.
12. Matsumura K, Mayama T, Lin H, Sakamoto Y, Ogawa K, Imanaga I. Effects of cyclic AMP on the function of the cardiac gap junction during hypoxia. Exp Clin Cardiol 2006;11:286-93.
13. Imanaga I. Role of the cardiac gap junctions in impulse propagation – with special reference to the transitional region between different heart tissues. Exp Clin Cardiol 1997;2:5-12.
14. Parmley WW, Rabinowitz B, Chuck L, Bonorris G, Katz JP. Comparative effects of sotalol and propranolol on contractility of papillary muscles and adenyl cyclase activity of myocardial extracts of cat. J Clin Pharmacol New Drugs 1972;12:127-35.
15. Goto M, Imanaga I. Roles of the cell membrane in producing cardiac arrhythmia; with special reference to the ectopic pacemaker potential and block of excitation conduction produced by aconitine. Jpn Circ J 1967;31:1555-60.
16. Schmidt H, Schmitt O. Effect of aconitine on the sodium permeability of the node of Ranvier. Pflugers Arch 1974;349:133-48.
17. Nilius B, Boldt W, Benndorf K. Properties of aconitine-modified sodium channels in single cells of mouse ventricular myocardium. Gen Physiol Biophys 1986;5:473-84.
18. Sawanobori T, Hirano Y, Hiraoka M. Aconitine-induced delayed afterdepolarization in frog atrium and guinea pig papillary muscles in the presence of low concentrations of Ca^{2+}. Jpn J Physiol 1987;37:59-79.
19. Maurer P, Weingart R. Cell pairs isolated from adult guinea pig and rat hearts: Effects of $[Ca^{2+}]i$ on nexal membrane resistance. Pflugers Arch 1987;409:394-402.
20. Noma A, Tsuboi N. Dependence of junctional conductance on proton, calcium and magnesium ions in cardiac paired cells of guinea-pig. J Physiol 1987;382:193-211.
21. Toyama J, Sugiura H, Kamiya K, Kodama I, Terasawa M, Hidaka H. Ca(2+)-calmodulin mediated modulation of the electrical coupling of ventricular myocytes isolated from guinea pig heart. J Mol Cell Cardiol 1994;26:1007-15.
22. Firek L, Weingart R. Modification of gap junction conductance by divalent cations and protons in neonatal rat heart cells. J Mol Cell Cardiol 1995;27:1633-43.
23. Tribulova N, Manoach M, Varon D, Okruhlicova L, Zinman T, Shainberg A. Dispersion of cell-to-cell uncoupling precedes low K^+-induced ventricular fibrillation. Physiol Res 2001;50:247-59.
24. Okruhlicova N, Tribulova N, Misejkova M, et al. Gap junction remodelling is involved in the susceptibility of diabetic rats to hypokalemia-induced ventricular fibrillation. Acta Histochem 2002;104:387-91.
25. Tribulova N, Okruhlicova L, Novakova S, et al. Hypertension-related intermyocyte junction remodelling is associated with a higher incidence of low-K(+)-induced lethal arrhythmias in isolated rat heart. Exp Physiol 2002;87:195-205.
26. Hekimian G, Khandoudi N, Feuvary D, Beigelman PM. Abnormal cardiac rhythm in diabetic rats. Life Sci 1985;37:547-55.
27. Bakth S, Arena J, Lee W, et al. Arrhythmia susceptibility and myocardial composition in diabetes. Influence of physical conditioning. J Clin Invest 1986;77:382-95.
28. Yang Q, Kiyoshige K, Fujimoto T, et al. Signal-averaging electrocardiogram in patients with diabetes mellitus. Jpn Heart J 1990;31:25-33.
29. Imanaga I, Hiriosawa N, Hai L, Sakamoto Y, Matsumura K, Mayama T. Phosphorylation of connexin 43 and regulation of cardiac gap junction. In: DeMello WC, Janse MJ, eds. Heart Cell

Coupling and Impulse Propagation in Health and Disease. Boston: Kluwer Academic Publishers, 2002:185-205.

30. Kato R, Ikeda N, Yabek SM, Kannan R, Singh BN. Electrophysiologic effects of the levo- and dextrorotatory isomers of sotalol in isolated cardiac muscle and their in vivo pharmacokinetics. J Am Coll Cardiol 1986;7:116-25.

31. Miyachi E, Manoach M, Uchiyama H, Watanabe Y. Is cyclic AMP involved in the defibrillating effect of sotalol? Life Sci 1995;57:PL393-9.

32. Manoach M, Tribulova N, Imanaga I. The protective effect of D-sotalol against hypoxia-induced myocardial uncoupling. Heart Vessels 1996;11:281-8.

33. Uchiyama H, Manoach M, Miyachi E, Watanabe Y. Sotalol facilitates spontaneous ventricular defibrillation by enhancing intercellular coupling. An entirely new mechanism for its antiarrhythmic action. Heart Vessels 1995;10:185-9.

34. Lompre AM, Anger M, Levitsky D. Sarco(endo)plasmic reticulum calcium pumps in the cardiovascular system: Function and gene expression. J Mol Cell Cardiol 1994;26:1109-21.

35. Voss J, Jones LR, Thomas DD. The physical mechanism of calcium pump regulation in the heart. Biophys J 1994;67:190-5.

36. Koss KL, Kranias EG. Phospholamban: A prominent regulator of myocardial contractility. Circ Res 1996;79:1059-63.